I J M R
International Journal of Microbiology Research
ISSN: 0975-5276 & E-ISSN: 0975–9174, Vol. 3, Issue 3, 2011, pp-157-163
Available online at http://www.bioinfo.in/contents.php?id=27

MICROBIAL GAS SENSING PROPERTY OF BACILLUS *SUBTILIS* WITH MIXED METAL CATALYST $MGFE_2O_4$

CHAUGULE V.V.[1] AND BANGALE S.V.[2]
[1]Determent of Microbiology, Miraj Mahavidyalaya, Miraj, Sangli 416416 MS. India
[2]Determent of Chemistry, Miraj Mahavidyalaya, Miraj, Sangli 416416 MS. India
*Corresponding Author: Email- bangale_sv@rediffmail.com

Received: December 09, 2011; Accepted: December 15, 2011

Abstract- Semiconductive nanoparticles of bacteria as *Bacillus subtilis* with catalyst MgFe2O4 biofilm was synthesized by using solution combustion technique. The process was convenient, environment friendly and efficient method. Materials were characterized by TG/DTA, XRD, and TEM. Thick biofilm of *Bacillus subtilis* $MgFe_2O_4$ was measured by exposing it to reducing economical gases. It was found that the *Bacillus subtilis* was sensors exhibited various sensing responses to these gases at different operating temperature. The sensor exhibited a fast response and a good recovery. The biofilm can be used as a new type of gas-sensing material which has a high sensitivity and good selectivity to various gases at low ppm.
Keyword- Nanostructure *Bacillus subtilis* with catalyst $MgFe_2O_4$, XRD, SEM, TEM, Gas sensor

Introduction

Bacillus subtilis, is refer as hay bacillus or grass bacillus, is a Gram-positive bacteria, has showing positive for catalase production. The habitat of *Bacillus subtilis* is soil. All *Bacillus* spp. Including B. *subtilis* is rod-shaped; allow tolerating extreme environmental conditions due to their endospore. Unlike several other well-known species, *B. subtilis* has historically been classified as an obligate aerobe, though recent research has demonstrated that this is not strictly correct.

B. subtilis has approximately 4,100 genes. Of these, only 192 were shown to be indispensable; another 79 were predicted to be essential as well. A vast majority of essential genes were categorized in relatively few domains of cell metabolism, with about half involved in information processing, one-fifth involved in the synthesis of cell envelope and the determination of cell shape and division, and one-tenth related to cell energetics [34]. *B. subtilis* has proven highly agreeable to genetic Engineering , and has become widely assume as a key model bacteria for vitro and vivo studies, sporulation, which is one example of cellular differentiation. It is flagellated, move *B. subtilis* quickly in liquids due to their flagella. It can biodegrade some explosives and can convert into harmless compounds such as nitrogen, carbon dioxide, and water. Therefore, the view *Bacillus subtilis* is used for gas sensing property in our study.

The size of Bacillus subtilis is just about 0.2µm therefore *Bacillus subtilis* act as best nanoparticle and consequently used for study along with $MgFe_2O_4$ used as a catalyst to sense the various gases. Spinal of the type M^{2+} $M_2^{3+}O_4$ attract the research interest because of their versatile practical application [1-2]. Spinel ferrites with the general formula AFe_2O_4 (A = Mn, Co, Ni, Mg, or Zn) are very important magnetic materials because of their interesting magnetic and electrical properties with chemical as well as thermal stabilities [3]. Magnesium ferrite ($MgFe_2O_4$) is one of the most important ferrites. It has cubic structure as normal spinel-type and is a soft magnetic n-type semiconducting material, which finds a number of applications in heterogeneous catalysis, adsorption, sensors, and in magnetic technologies [4-5]. Recently, nanostructures of magnetic materials have received more and supplementary attention due to their novel material properties that are significantly different from those of their bulk counterparts [6-9]. Current years have been increased interests in study the gas sensing properties of ferrites [10-12]. Gopal reddy et al. reported the response of copper ferrite ($CuFe_2O_4$) and zinc ferrite ($ZnFe_2O_4$) for hydrogen sulfide (H_2S) and that of nickel ferrite ($NiFe_2O_4$) for chlorine gas (Cl_2) [10]. One of the present authors (Y-L.Liu) was confirmed that $ZnFe_2O_4$ gas sensor has sensing properties for H_2S gas [11].Magnesium ferrite ($MgFe_2O_4$) is one of the important ferrites with spinel structure [13]. It is used as a catalyst [14] and humidity sensor [15]. It is also an n-type semiconductor with the band gap of 2.18V [16].

The need for a novel gas sensor capable of providing reliable operation in harsh environment is now greater than ever. Such sensors find a range of applications, including the monitoring of traffic pollutants or food quality with specially designed electronic noses [17-18]. Gas sensors based on metal oxides are commonly used in the monitoring of toxic pollutants and can provide the necessary sensitivity, selectivity and stability required by

such system [19]. Commonly used oxides include zinc oxide, titanium dioxide, iron oxide, tungsten oxide and tin oxide. These materials have successfully been employed to detect a range of gas vapours, particularly ethanol, methanol and propanol [20-21].

Among various materials used for sensing application, ferrite is used as a good class of sensing materials. But they suffer a drawback of being at higher temperature [22]. Consequently, it is interesting to investigate the gas-sensing properties of $MgFe_2O_4$. The gas sensing efficiency of the materials depends on its microstructural properties which are related to its method of preparation, the later plays a very important role with regard to the chemical, structural and properties of a spinel ferrite. $MgFe_2O_4$ is routinely synthesized by combustion method of precursors zinc nitrate, magnesium nitrate and glycine as fuel [23]. Some alternative number of wet methods including co-precipitation [24], sol-gel [25], micro-emulsions [26], oxidation techniques [27] and hydrothermal synthesis [28] has been employed for preparation of oxide. An ideal process should be environmentally friendly and should be as simple as possible. A novel preparation technique of nanomaterial combustion synthesis at ambient conditions has been developed to prepared nanosized compounds. It was a high-yielding, low-cost and facile synthesis method.

In this study, the powder of nanoparticles Bacillus subtilis was prepared and mixed with $MgFe_2O_4$ nanoparticles. The $MgFe_2O_4$ nanoparticle was synthesized by novel combustion reaction. One of our aims is to develop a general synthesis method and explore the gas sensing properties of Bacillus *subtilis* with catalyst $MgFe_2O_4$ which act as nanopowder. The grain size of $MgFe_2O_4$ is about 15-35nm and size of *Bacillus subtilis* 0.2μ. Furthermore, we found that the Bacillus subtilis with catalyst MgFe2O4 biofilm act as gas sensor and has possessed excellent gas-sensing responses to various reducing gases. The process has convenient, environment friendly, inexpensive and efficient. The discovery could aid that, this is low cost process carried out at room temperature particularly for the detection of ammonia gas.

Experimental

Isolation of *Bacillus subtilis*

For isolation of *Bacillus subtilis*, soil one of the raw materials was used because soil is the chief source for all microorganisms including Bacillus subtilis. One loop full sample from diluted soil was streaked on sterilized Nutrient agar plate; Plate was incubated at 37^{0}C for 24 hrs. After 24hrs dry and off white coloured colonies was selected for the confirmation of Bacillus subtilis.

Confirmation of *Bacillus subtilis*

Isolated *Bacillus subtilis* was confired by biochemical tests. The isolated colony was showing positive results for number of biochemical tests which was indicating presence of Bacillus subtilis.

Enrichment of *Bacillus subtilis*

The confirmed colony was streaked on another nutrient agar plates for enrichment purpose. All plates were incubated at 37^{0}C for 24 hrs. After 24hrs of incubation, aseptically scrub the growth of Bacillus subtilis in distilled water. The growth was then centrifuged to get pellet of Bacillus subtilis.

Powder preparation of *Bacillus subtilis*

The pellet of Bacillus subtilis was allowed to dry to get powder and powder directly used which act as nanoparticles. The size of Bacillus subtilis is in μm, thus Bacillus subtilis act as best nanopartical was used in study.

Powder preparation for $MgFe_2O_4$

In this study polycrystalline $MgFe_2O_4$ powder was prepared using combustion technique. The materials used as precursors were magnesium nitrate hexahydrate Mg $(NO_3)_2.6H_2O$, iron nitrate hexahydrate Fe $(NO_3)_26H_2O$ and glycine (all these were purchased from AR Grade of Qualigen fine Ltd. India). All of them were high pure with their purity (99.9%, 98%, and 99.9% respectively). Glycine possessing high heat combustion ability. It is an organic fuel providing a platform for redox reactions during the course of combustion. Initially the magnesium nitrate, iron nitrate and glycine were taken in the proportion of 1:1:4 respectively. These proportions were dissolved in a beaker and slowly stirring by glass rod, till clear solution was obtained. Then formed solution was evaporated on hot plate in the temperature range of 70^{0}C to 80^{0}C resulting thick gel. The gel was kept on a hot plate for auto combustion and heated in the temperature range of 170^{0}C to 180^{0}C. The nanocrystalline $MgFe_2O_4$ powder was formed within few minutes and it was sintered at about 500^{0}C, 600^{0}C, 700^{0}C, and 800^{0}C for about 4h, it gives brown colour shining powder of nanocrystalline $MgFe_2O_4$[29].

Characterization of MgFe2O4 Techniques

The prepared samples were characterized by TG/DTA thermal analyzer (SDT Q600 V 20.9 Build 20), XRD Philips Analytic X-ray B.V. (PW-3710 Based Model diffraction analysis using Cu-K_α radiation), A JEOL JEM–200 CX transmission electron microscope was operating at 200 kV for the said analysis.

Thick Film Preparation

The thixotropic paste of powder form of nanocrystalline *Bacillus subtilis* and $MgFe_2O_4$ was screen printed on a glass substrate in desired patterns. The films prepared were fired at 37^{0}C for 4h. Silver contact was made by vacuum evaporation for electrical measurements.

Fabrication and analysis of gas sensors

The sensing performance of the sensors was examined using a "static gas-sensing system. Electrical feeds were used through the base plate. The heating wire was fixed on the base plate to heat the sample up to specific temperatures, which test required operating temperatures. The current passing through the heating element was monitored using relay with adjustable ON and OFF switch at time intervals. Cr-Al thermocouple was used to sense the operating temperature of the

sensors. The output of the thermocouple was connected to digital temperature indicators. Gas inlet valve was fitted at one port of the base plate. The required gas concentration inside the static system was achieved by injecting known volume of test gas using a gas-injecting syringe. Constant voltage was applied to the sensors, and current was measured by a digital Pico-ammeter. Air was allowed to pass into the glass dome after every gases exposure cycle.

Result and Discussion

Spinel structure and formation analysis

The TG curve shown in Fig. 1 indicating a minor weight loss step (20%) from 30 up to about 270^{0}C and two major weight loss steps from 270 to 455^{0}C (60%). No further weight loss was observed up to 1000^{0}C. The minor weight loss was related to the loss of moisture and trapped solvent (water and carbon dioxide) in the as-spun $MgFe_2O_4$ nanopowder, whereas the major weight loss was due to the combustion of organic matrix. On the DTA curve, main exothermic peaks were observed at ~290 and ~ 450^{0}C, suggesting the thermal events related to the decomposition of Mg and Fe nitrates along with the degradation by dehydration on the nanopowder, which was confirmed by a dramatic weight loss in TG curve at the corresponding temperature range (270–455^{0}C). The plateau formed between 455 and 1000^{0}C on the TG curve was indicated the formation of crystalline $MgFe_2O_4$ as the decomposition product. It was confirmed by XRD and FT-IR analyses as showed in Figs. 2 and 5 respectively and represented by following reactions (1, 2).

$$2C_2NH_3O_2 + (9/2)\ O_2 \rightarrow N_2\uparrow + 4CO_2\uparrow + 5H_2O\uparrow \quad (1)$$

$$Mg(NO_3)_3 + Fe(NO_3)_3 + 4C_2H_5NO_2 \rightarrow MgFe_2O_4 + 8CO_2\uparrow + 10H_2O\uparrow + 5N_2\uparrow \quad (2)$$

XRD study

The XRD patterns of the calcined $MgFe_2O_4$ are shown in Fig. 2. All of the main peaks are indexed as the spinel $MgFe_2O_4$ in the standard data (JCPD No: 88-1935). The average crystallite sizes of $MgFe_2O_4$ samples were calculated from X-ray line broadening of the reflections of (220), (311), (400), (511), and (440) using Scherrer's equation (i.e., $D = 0.89k/(\beta \cos\theta)$, where k is the wavelength of the X-ray radiation, K is a constant taken as 0.89, h the diffraction angle, and b is the full width at half-maximum **[30]** , and were found to be 16 ± 4, 18 ± 1, 25 ± 2, and 26 ± 3 nm for the samples of $MgFe_2O_4$ calcined at 500, 600, 700, and 800^{0}C, respectively.

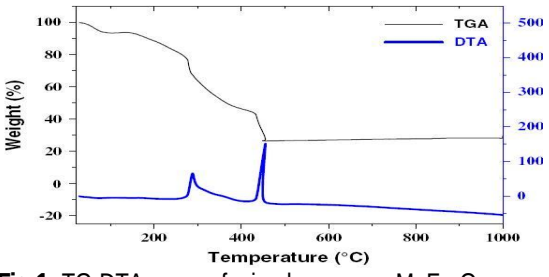

Fig.1- TG-DTA curve of mixed precursor $MgFe_2O_4$

Particle size distribution studies

Fig. 3 plotted out by using dynamic light scattering techniques. (DLS *via* Laser input energy of 632 nm) It was observed that magnesium iron oxide nanoparticles have narrow size distribute within the range of about 10-15 nm. Which well match with calculated value and was calculated, it from Debye-Scherrer equation.

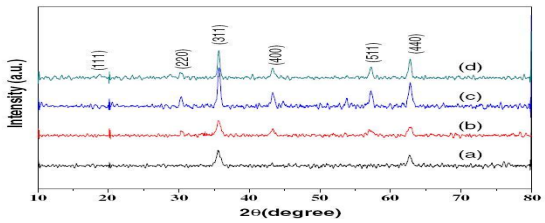

Fig.2- XRD pattern of calcinied mixed precursor $MgFe_2O_4$ at a - 5000C, b- 6000C, C-7000C and d- 800^{0}C in air for 4 h.

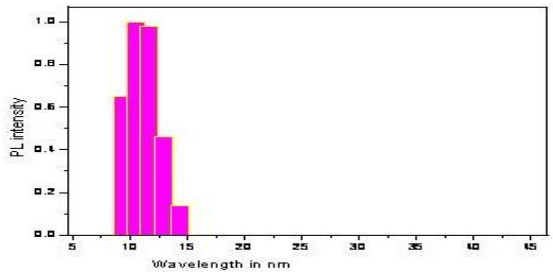

Fig.3- Particle size distribution studies

TEM studied

The detailed morphology and crystalline structure of the $MgFe_2O_4$ calcined at 700 and 800^{0}C for 4 h were further investigated by TEM, and the TEM bright-field images with corresponding selected-area electron diffraction (SAED) patterns of these two samples are shown in Fig.4. From the TEM bright field images it was clearly seen that both samples consisted of packed $MgFe_2O_4$ particles or crystallites with particle sizes of ~10–20 and 25–80 nm in diameter for the samples of 700^{0}C-calcined and 800^{0}C-calcined, respectively. It is seen that the particle sizes of $MgFe_2O_4$ contained in the calcined $MgFe_2O_4$ are quite uniform. Synthesized powder was showing standard data (JCPDS: 88-1935). The diffraction rings was identified as the (111), (220), (311), (400), (422), (511), and (440) planes. This concurs with the results of XRD presented in Fig. 2.

FT-IR Studied

The formation of spinel $MgFe_2O_4$ structure in the calcined $MgFe_2O_4$ was further supported by FT-IR spectra (Fig.5). Here, consider two ranges of the absorption bands: 4000–1000 and 1000–400 cm^{-1} as suggested by previously published studies [31-32]. In the range of 4000–1000 cm^{-1}, vibrations of CO_3^{2-} and moisture were observed. The intensive band at~-1627 cm^{-1} is due to O–H stretching vibration interacting through H bonds. The band at ~ 2920 cm^{-1} is C–H asymmetric stretching vibration mode due to the $–CH_2–$ groups of the long aliphatic alkyl groups. The υ(C=O)

stretching vibration of the carboxylate group (CO_2^{2-}) was observed around 1380 cm^{-1} and the band at ~1016 cm^{-1} was corresponded to nitrate ion traces. Therefore the CO_3^{2-} and CO_3^{-} vibrations disappeared when calcinations temperature was increased. In the range of 1000–400cm^{-1}, a typical metal–oxygen absorption band for the spinel structure of the ferrite at ~560 cm^{-1} was observed in the FT-IR spectra of all calcined $MgFe_2O_4$ samples. This band strongly suggests the intrinsic stretching vibrations of the metal (Fe ↔ O) at the tetrahedral site [3]

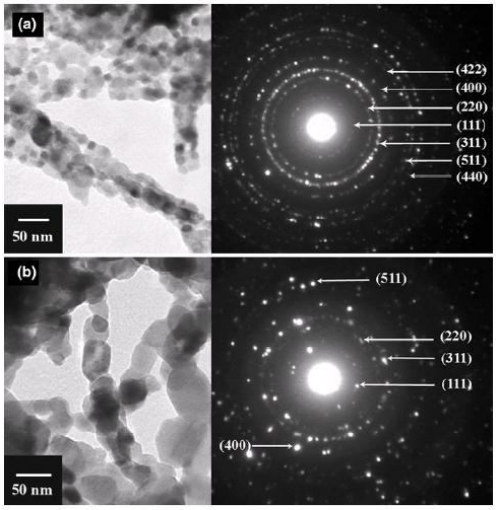

Fig.4- TEM images with corresponding SAED patterns of the $MgFe_2O_4$ samples Calcined in air for 4 h at a 700^{0}C and b 800^{0}C.

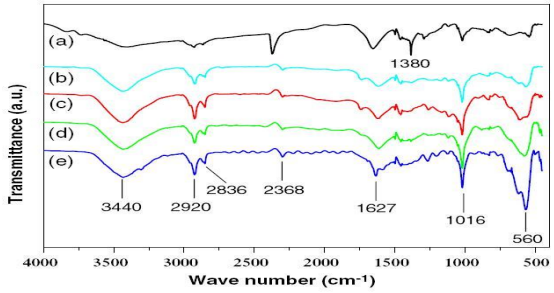

Fig. 5- FT-IR spectra of the $MgFe_2O_4$ composite samples calcined in air for 4 h at different temperatures. a - As-spun, b -500^{0}C, c - 600^{0}C, d - 700^{0}C, and e - 800^0 C

Electrical properties

I-V characteristics of thick film nanoparticles Bacillus subtilis and $MgFe_2O_4$

Fig.6 depicts I-V characteristics of nanoparticles Bacillus subtilis with $MgFe_2O_4$ biofilms. From the symmetrical I-V characteristics it was clear that the silver contacts on the bio-films were ohmic in nature.

Electrical conductivity

Fig.7 shows the variation of log (conductivity) with temperature. The conductivity values of sample increase with operating temperature. The increase in conductivity with increasing temperature could be attributed to negative temperature coefficient of resistance and semiconducting nature of *Bacillus subtilis* with $MgFe_2O_4$ bio-film. From fig. 7, it was observed that the electrical conductivities of the *Bacillus subtilis* with MgFe2O4 bio-films were nearly linear within the temperature range from 30- 40^{0}C in air ambient.

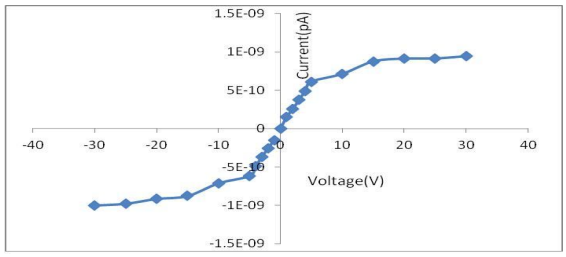

Fig.6- I-V characteristics of the biosensor

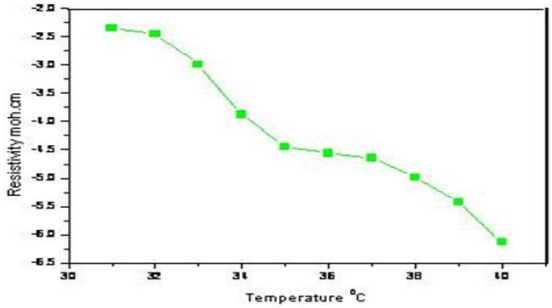

Fig.7- Resistivity Variation of Bacillus subtilis with MgFe2O4 bio-film with reciprocal operating temperature (K^{-1})

Sensing performance of the sensor

Measurement of gas response, selectivity and recovery time

Gas response (S) is defined as the ratio of the change in conductance of the sensor on exposure to the target gas for the original conductance in air. The relation for S is as:

$$S = \frac{G_g - G_a}{G_a}$$

Where, G_a and G_g were the conductance of sensor in air and in target gas medium, respectively.

Selectivity or specificity was defined as the ability of a sensor to respond for a certain gas in the presence of other gases.

The time taken for the sensors to attain 90% of the original conductance was the recovery time.

Sensing performance of thick film Bacillus subtilis with $MgFe_2O_4$ bio-film

Effect of operating temperature

Table 1 and Fig. 8 depict the response of Bacillus subtilis with Mg2Fe2O4 bio-film to CO_2 (300 ppm) with various operating temperature. The largest response of nanaopartical thick Bacillus subtilis with Mg2Fe2O4 bio-film was observed to be 7.21% at 37^{0}C. The CO_2 response at 37^{0}C temperature was expected to be monitored by adsorption of moisture on the Bacillus subtilis, $MgFe_2O_4$ film. The cumulative effect would decrease the film resistance, giving a response to CO_2 gas at 37^{0}C. Except 37^{0}C, there would be no more oxygen adsorption. Therefore, the oxygen adsorption-desorption mechanism is quit employed to sense the CO_2 gas at other temperatures.

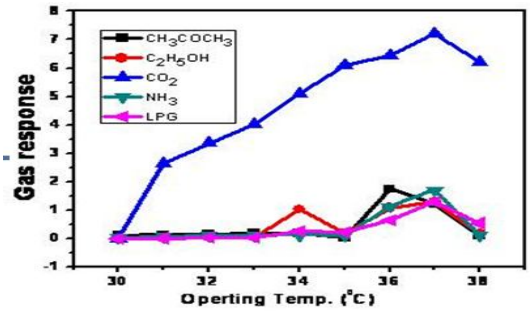

Fig.8- Graphical variations of various gas responses to Bacillus subtilis with $MgFe_2O_4$ thick bio-film with different operating temperatures

Table 1- Variations of various gas responses to Bacillus subtilis with $MgFe_2O_4$ thick bio-film with operating temperatures

Temperature	Acetone	Ethonal	CO2	NH3	LPG
38	0.11	0.1732	6.225	0.124	0.5551
37	1.213	1.302	7.21818	1.7065	1.2951
36	1.746	1.08823	6.4312	1.13285	0.6493
35	0.0505	0.178	6.08695	0.11	0.24
34	0.1875	1.03428	5.1011	0.1355	0.2589
33	0.1789	0.05567	4.0104	0.1324	0.03174
32	0.15678	0.05302	3.3547	0.1287	0.02892
31	0.1354	0.04092	2.6589	0.0721	0.01489
30	0.120	0.024	0.012	0.0573	0.01

Effect of CO_2 gas concentration at 37^{0}C (Active Region)

The variation of gas response of the *Bacillus subtilis* with $MgFe_2O_4$ bio-film sample with CO_2 gas concentration at 37^{0}C is represented in Fig.9. This film was exposed to varying concentrations of CO_2 gas. For thick bio-film of *Bacillus subtilis* $MgFe_2O_4$, the response values were observed to increase continuously with increasing the gas concentration up to 300 ppm at 37^{0}C. The rate of increase in response was relatively larger up to 300 ppm, but smaller during 30 and 1200 ppm. Thus, the active region of the sensors would be up to 300 ppm. At lower gas concentration, the unimolecular layer of gas molecules would be formed on the surface of the sensor which could interact more actively giving larger response. The multilayer of the gas molecules on the sensor surface, would result into saturation in response beyond 300 ppm gas at higher gas concentration,

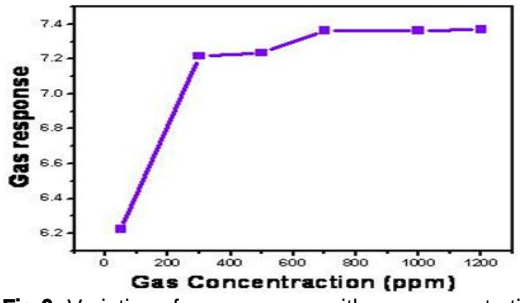

Fig.9- Variation of gas response with gas concentrations for the Bacillus subtilis with $MgFe_2O_4$ bio-film.

Selectivity for CO_2 against various *gases*

Fig.10. depicts the selectivity of the Bacillus subtilis $MgFe_2O_4$ bio-sensor for CO_2 (300 ppm) gas at 37^{0}C. The sensor showed high selectivity to CO_2 at 300 ppm and 37^{0}C temperature against other gases as ethanol, acetone, LPG and CO_2 but these gases showed high selectivity at 1200 ppm.

Response and recovery of the sensor

Fig.11 depicts the response and recovery of the Bacillus subtilis $MgFe_2O_4$ biosensor. The response was quick (~ 20 s) to 300 ppm of CO_2, while the recovery was considerably fast (~ 60 s). A negligible quantity of the surface reaction product and its volatility explain its quick response to CO_2 and fast recovery to its initial chemical status.

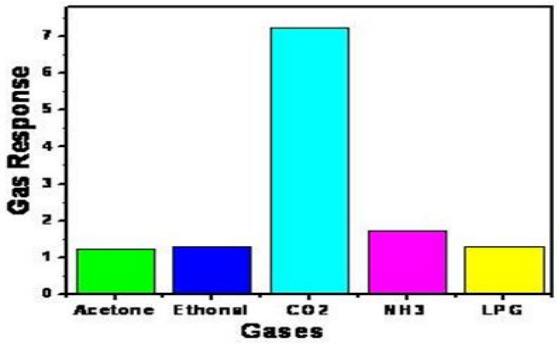

Fig. 10- Selectivity of Bacillus subtilis with $MgFe_2O_4$ thick biofilm among various gases

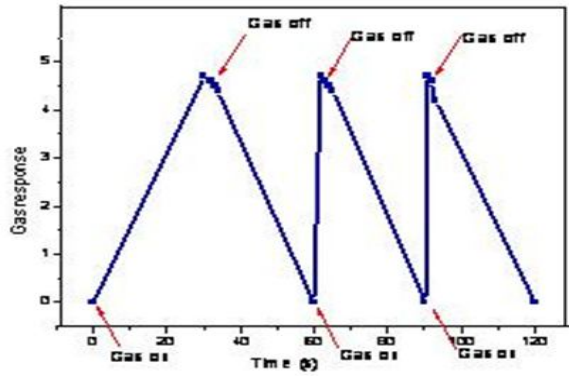

Fig. 11- Response and recovery of the biosensors

Response at various temperatures

The Bacillus subtilis $MgFe_2O_4$ thick bio-films cause the formation of intergrain boundaries of Bacillus subtilis-$MgFe_2O_4$-Bacillus subtilis-$MgFe_2O_4$ grains. The exposed all gases molecule captures the lattice oxygen from the surface of the film at various temperature. This would result the oxygen deficiency carried out by ethanol, acetone, LPG and CO_2 gases in the bulk of the material preferably at the surface. The semiconductivity in Bacillus subtilis $MgFe_2O_4$ may be due to large oxygen deficiency. The increase in the conductivity of Bacillus subtilis $MgFe_2O_4$ thick bio-film could be attributed to the charge-carrier generation mechanism resulted from the electronic defects due to nanostructured size of the grains. These generated electrons and the donor level in the energy band gap of Bacillus subtilis $MgFe_2O_4$ will contribute to increase in conductivity. This results in

increasing the conductance of the film at various temperatures.

Conclusion

- Bacillus subtilis use as nano crystalline material synthesized by centrifuged and dried method and nanocrystalline $MgFe_2O_4$ has been synthesized by self combustion route. This synthesis route may be used for the synthesis of bacteria and other metal oxide.
- These nanoparticles $MgFe_2O_4$ which show good I-V characteristics with ideal semiconducting nature.
- Among all other additives tested, Bacillus subtilis $MgFe_2O_4$ thick bio-film is outstanding in promoting the CO_2 gas.
- Bacillus subtilis $MgFe_2O_4$ thick bio-film to be optimum and showed highest response to CO_2 at 37^0C.
- (V)The biosensor showed very rapid response and good recovery for CO2 gas.
- The biosensor has good selectivity to CO_2 against ethanol, acetone, NH_3 and LPG also.

Acknowledgement

The author vinay chaugule is thankful to IIT Bombay for providing the TEM facility and Sachin Bangale for his help during this research work.

References

[1] Sugimoto M. (1999) *J.Am.Ceram.Soc.* [82, 269].
[2] Liu Y., Liu Z.M., Yang Y., Yang H.F., Shen G.L., Yu R.Q. (2005) *Sensors ans Actuators B* , 107, 600-604.
[3] Hankare P.P., Jadhav S.D., Sankpal U.B., Patil R.P., Sasikala R., Mulla I.S. (2009) *Alloys and Compounds*, 488, 270-272.
[4] Willey R.J., Noirclerc P., Busca G. (1993) *Chem.Eng.Commun*. 123.
[5] Oliver S.A.,Willey R.J.,Hamdeh H.H., Oliveri G., Busca G. (1995) *Scr.Mater*., 33, 1695.
[6] Wu W., He Q., Jiang C. *(*2008) *Nanoscale Res. Lett.*, 3, 397.
[7] Hua Z.H., Chen R.S., Li C.L., Yang S.G., Lu M., Gu X.B., Du Y.W. (2007) *J. Alloys Compd*., 427, 199.
[8] Corr S.A., Rakovich Y.P., Gun'ko Y.K. *(*2008) *Nanoscale Res. Lett.,* 3, 87.
[9] Lai Z., Xu G., Zheng Y. (2007) *Nanoscale Res. Lett*., *2,* 40.
[10] Gopal Reddy C.V., Manorama S.V, Rao V.J., (2000) *J.Mater. Sci.Lett*. [19, 775].
[11] Xinshu N., Yanli L., X.Jiaqiang (2002) *Chin.Funct.Mater*. , 33, 413.
[12] Satyanarayana L., Madhusudan K. Reddy, Sunkara V.M. (2003) *Mater.Chem.Phys*. 82, 21.
[13] Liu C., Zou B., Rondinone A.J., Zhang Z.J. (2000) *J.Am.Chem.Soc*. 122, 6263.
[14] Busca G., Finocchio E., Lorenzelli V., Trombetta M., Rossini S.A. (1996) *J.Chem.Soc. Faraday Trans*., 92, 4687.
[15] Shimizu Y., Arai H., Seiyama T. (1985) *Sens. Actuators*, 7*,* 11.
[16] Benko F.A., Koffyberg F.P. (1986) *Mater.Res.Bull*. 21, 1183.
[17] Sugimoto M (1999) *J.Am.Ceram.Soc*.82, 269-280.
[18] Kamble R.B., Mathe V.L. (2008) *Sensors and Actuatora B* 131, 205-209.
[19] McMichael R.D., Shull R.D., Swartzendruber L.J., Bennett L.H., Watson R.E. (1992) *J. Magn. Magn.Mater.* 11, 29-33.
[20] Gopal Reddy C.V., Manorama S.V., Rao V.J. (2000) J.Mater.Sci.Lett. , 9, 775-778.
[21] Chen N.S., Yang X.J., Liu E.S., Huang J.L. (2000) *Sens. Actuators B* 66, 178-180.
[22] Rezlescu E., Popa P.D. (2006) *N.Rezlescu 8*, 1016.
[23] Khetre S.M., Jadhav H.V., Jagdale P.N., Bangale S.V., Bamane S.R. (2011) *Advances in Applied Science Research*, *2, (2)* , 252-259.
[24] Kodama T., Wada Y., Yamamoto T., Tsuji M (1995) J. Mater. Chem 5, 1413.
[25] Hirano S, Yogo T, Kikuta K, Asai E, K.Sugiyama, Yamamoto H (1993) *J. Am. Ceram. Soc*., 76, 1788.
[26] Hochepied J.F., Bonville P., Pileni M.P. (2000) *J.Phys.Chem. B*, 104,905.
[27] Kiyama M. Bull (1978) *Soc.Jpn*, 51, 134.
[28] Verma S., Joy P.A., Khollam Y.B., Potdar H.S., Deshpande S.B. (2004) *Mater.Lett*. 58, 1092.
[29] Bangale S.V., Khetre S.M. and Bamane S.R. (2011) *Advances in Applied Science Research*, 2, 252-259.
[30] Cullity B.D., Stock S.R. (2001) *Elements of X-ray Diffraction* (Prentice Hall, NJ.)
[31] Huang Y., Tang Y., Wang J., Chen Q. (2006) *Mater. Chem. Phys*. 97, 394.
[32] Pradeep A., Chandrasekaran G. (2006) *Magnesium Mater. Lett.* 60, 371.
[33] Rao G.V.S., Rao C.N.R, Ferraro J.R. (1970) *Appl. Spectrosc*. 24, 436.
[34] Kobayashi K., Ehrlich S.D., Albertini A., Amati G., Andersen K.K., Arnaud M., Asai K., Ashikaga S., Aymerich S., Bessieres P., Boland F., Brignell S.C., Bron S., Bunai K., Chapuis J., Christiansen L.C., Danchin A., Débarbouille M., Dervyn E., Deuerling E., Devine K., Devine S.K., Dreesen O., Errington J., Fillinger S., Foster S.J., Fujita Y., Galizzi A., Gardan R., Eschevins C., Fukushima T., Haga K., Harwood C.R., Hecker M., Hosoya D., Hullo M.F., Kakeshita H., Karamata D., Kasahara Y., Kawamura F., Koga K., Koski P., Kuwana R., Imamura D., Ishimaru M., Ishikawa S., Ishio I., Le Coq D., Masson A., Mauël C., Meima R., Mellado R.P., Moir A., Moriya S., Nagakawa E., Nanamiya H., Nakai S., Nygaard P., Ogura M., Ohanan T., O'Reilly M., O'Rourke M., Pragai Z., Pooley H.M., Rapoport G., Rawlins

J.P., Rivas L.A., Rivolta C., Sadaie A., Sadaie Y., Sarvas M., Sato T., Saxild H.H., Scanlan E., Schumann W., Seegers J.F., Sekiguchi J., Sekowska A., Séror S.J., Simon M., Stragier P., Studer R., Takamatsu H., Tanaka T., Takeuchi M., Thomaides H.B., Vagner V., van Dijl J.M., Watabe K., Wipat A., Yamamoto H., Yamamoto M., Yamamoto Y., Yamane K., Yata K., Yoshida K., Yoshikawa H., Zuber U., Ogasawara N. (2003) *PNAS, 100* (8), 4678-83.